BaZr$_{0.5}$Ti$_{0.5}$O$_3$: Lead-free relaxor ferroelectric or dipolar glass

C. Filipič, Z. Kutnjak, and R. Pirc

Jožef Stefan Institute, Jamova cesta 39, 1000 Ljubljana, Slovenia

G. Canu

Institute for Energetics and Interphases, National Research Council, via De Marini 6, I-16149 Genoa, Italy

J. Petzelt

Institute of Physics, Academy of Sciences of the Czech Republic, Na Slovance 2, 182 21 Praha 8, Czech Republic

Glassy freezing dynamics was investigated in BaZr$_{0.5}$Ti$_{0.5}$O$_3$ (BZT50) ceramic samples by means of dielectric spectroscopy in the frequency range 0.001 Hz–1 MHz at temperatures $10 < T < 300$ K. From measurements of the quasistatic dielectric polarization in bias electric fields up to ∼28 kV/cm it has been found that a ferroelectric state cannot be induced, in contrast to the case of typical relaxors. This suggests that—at least for the above field amplitudes—BZT50 effectively behaves as a dipolar glass, which can be characterized by a negative value of the static third order nonlinear permittivity. The relaxation spectrum has been analyzed by means of the frequency-temperature plot, which shows that the longest relaxation time obeys the Vogel-Fulcher relation $\tau = \tau_0 \exp[E_0/(T - T_0)]$ with the freezing temperature of 48.1 K, whereas the corresponding value for the shortest relaxation time is ∼0 K, implying an Arrhenius type behavior. By applying a standard expression for the static linear permittivity of dipolar glasses and/or relaxors the value of the Edwards-Anderson order parameter $q(T)$ has been evaluated. It is further shown that $q(T)$ can be described by the spherical random bond-random field model of relaxors.

I. INTRODUCTION

Relaxor ferroelectrics (relaxors) have long been attracting considerable attention in view of a number of special physical properties [1]: (i) broad frequency dependent peak in the complex dielectric permittivity; (ii) absence of spontaneous polarization and of global symmetry breaking down to lowest temperatures; (iii) clustering of elementary dipolar entities giving rise to polar nanoregions (PNRs), which appear at relatively high temperatures; (iv) broad distribution of relaxation times and divergence of the longest relaxation time, leading to ergodicity breaking and hence to freezing phenomena; and (v) a field-induced ferroelectric state can be achieved by cooling in a sufficiently high electric field along one or more symmetry directions. It should be noted that features (i)–(iv) also apply to a group of closely related disordered systems known as dipolar glasses; however, feature (v) is an inherent property of relaxors, and could thus be used to discriminate between relaxors and dipolar glasses in marginal cases. In fact, relaxors can exhibit either dipolar glass or ferroelectric nature depending on whether they are studied below the critical field line $E_c(T)$ or above [2].

The oldest and probably most widely studied relaxor is the disordered perovskite PbMg$_{1/3}$Nb$_{2/3}$O$_3$ (PMN) [3], but a vast number of other systems have been described over the years [4,5]. Recently the BaZr$_x$Ti$_{1-x}$O$_3$ (BZT) solid solution came into focus for two main reasons: First, it is lead free and thus environmentally more acceptable for possible applications, and second, zirconium is isovalent to titanium, suggesting that random fields are minimized, thus bringing BZT conceptually close to the case of magnetic spin glasses [6].

There have been several experimental investigations of BZT ceramics so far [7–17]. Maiti *et al.* studied the structure of BZT

for a number of compositions with different Zr content x, and found that BZT is a relaxor for $0.25 \lesssim x \lesssim 0.75$ [8,11]. Petzelt *et al.* [12,13] carried out an extensive broadband spectroscopy study of BZT and found that for a set of concentrations in the above range the relaxation time follows the Arrhenius rather than the Vogel-Fulcher law, and concluded that BZT should be classified as a dipolar glass rather than a relaxor. Similarly, Kleemann *et al.* [15] studied the nonlinear permittivity of BZT for $0.25 \leqslant x \leqslant 0.35$ and described the crossover from ferroelectric to relaxor and cluster glass behavior.

In recent first-principles-based theoretical work Akbarzadeh *et al.* [18] investigated the properties of BZT for the case $x = 0.5$. They observed the formation of PNRs and calculated several physical quantities such as the direct and the field-cooled susceptibility and the Edwards-Anderson order parameter. They found that random electric fields and random strains did not contribute significantly to their results, and also discussed the importance of antiferroelectric interactions between Ti-rich nanopolar clusters for the relaxor behavior. Meanwhile, Sherrington [6] discussed a microscopic model of BZT, which explicitly includes the interactions of Ti and Zr ions with neighboring ions, and found that BZT can be understood by mapping to a soft pseudospin glass.

In order to gain further insight into the properties of BZT in the relaxor regime and, in particular, to address the issue whether BZT could be classified as a relaxor or a dipolar glass, we have carried out a dielectric study of the quasistatic and dynamic behavior of BZT at $x = 0.50$. The concentration $x = 0.50$ was chosen because it lies in the middle of the presumed relaxor regime, and because the case $x = 0.50$ has been explicitly investigated in some theoretical [18–20] and experimental [10,21] studies.

Several criteria to discriminate between dipolar glasses and relaxors have been formulated in the past. From a microscopic point of view, it is clear that in dipolar glasses there may be some clustering of the elementary dipoles but the resulting PNRs will remain small, i.e., of the order of a few lattice constants. In relaxors, however, the PNRs can be large and their dipole moments may be affected by the applied electric field. This is reflected in the shape of the probability distribution of relaxation times $f(\tau)$, which can be extracted from the complex dielectric permittivity by means of the Tikhonov regularization method [22,23]. In dipolar glasses $f(\tau)$ has a single peak structure, whereas in relaxors a second peak appears at low temperatures, where the two peaks in relaxors are related to the flipping and breathing modes of the PNRs [24,25].

Another manifestation of relaxor behavior is the occurrence of square hysteresis loops for some symmetry directions of the field E, implying that a first order transition into a field-induced ferroelectric phase appears [26]. On further increasing the field amplitude a critical point in the E,T plane is reached. On the other hand, in dipolar glasses only slim hysteresis loops are observed and no critical point exists for any field direction and amplitude. Alternatively, one can monitor the static polarization on lowering the temperature in a field by the charge accumulation technique, and look for a first order jump of polarization at a threshold field [27]. Here we will apply this method to BZT50 in order to test whether it behaves as a normal relaxor or a dipolar glass.

II. EXPERIMENTAL DETAILS

The complex dielectric constant $\varepsilon^*(f,T) = \varepsilon' - i\varepsilon''$ was measured between 10 and 300 K in the frequency range 0.001 Hz $< f <$ 1 MHz using a Novocontrol Alpha High Resolution Dielectric Analyzer. The amplitude of the probing ac electric signal was 1 V/mm. The temperature was stabilized within ± 0.1 K using an Oxford Instruments continuous flow cryostat and an ITC4 temperature controller.

BZT powders with composition $x = 0.50$ were synthesised by conventional solid state reaction, with calcination at 1000 °C for 4 h. Dense ceramic samples were prepared by compacting the powder by cold isostatic pressing (1500 bars) and sintering the pellet at 1500 °C for 4 h. The obtained ceramics were single phase, with perovskite structure, with relative density over 98% compared to the theoretical density, and grain size of a few microns [13].

Ceramics samples had a diameter of typically 6 mm and thickness of 0.25 mm. Gold electrodes were sputtered on the disk faces.

The temperature dependence of the field-cooled (FC) and zero-field-heated (ZFH) (after field-cooling) quasistatic dielectric polarization was measured using the charge-accumulation technique (the external bias field applied to a sample was up to 28 kV/cm) using a Keithley 617 programmable electrometer [28]. The temperature dependence of the field-cooled (FC) dielectric polarization was determined during cooling the sample with the rate of −1.6 K/min. An analogous rate (+1.6 K/min) was used when heating the sample after external bias voltage had been removed from the
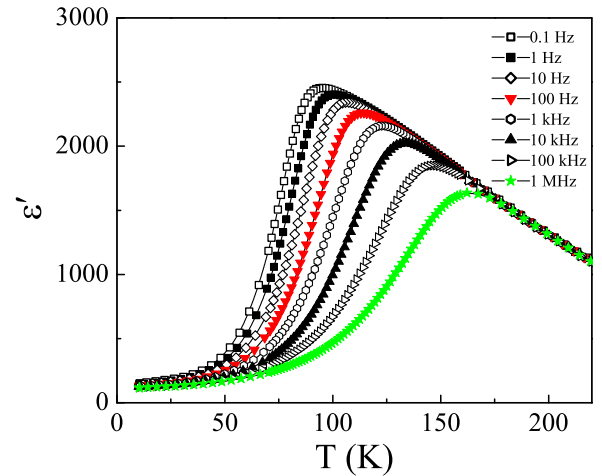

FIG. 1. Temperature dependence of the real part of the complex dielectric constant ε' in BZT50 at various frequencies, showing a typical relaxor behavior.

sample at 10 K, and the zero-field-heated (ZFH) quasistatic dielectric polarization was determined.

Polarization vs electric field $P(E)$ loops were measured using a Sawyer-Tower bridge. The external field was applied to the sample from 0 up to 28 kV/cm with a rate of approximately 0.002 Hz. The polarization measurements were performed always after cooling the sample from room temperature to a desired temperature (at zero electric field) with the cooling rate of −1.6 K/min.

III. DATA ANALYSIS AND DISCUSSION

The temperature dependence of ε' and ε'', measured at different frequencies (0.001 Hz–1 MHz), is shown in Figs. 1 and 2, respectively. The figures show a typical behavior, as found in dipolar glasses or relaxors, in a broad temperature interval, where the maxima of ε' and ε'' for a set of selected
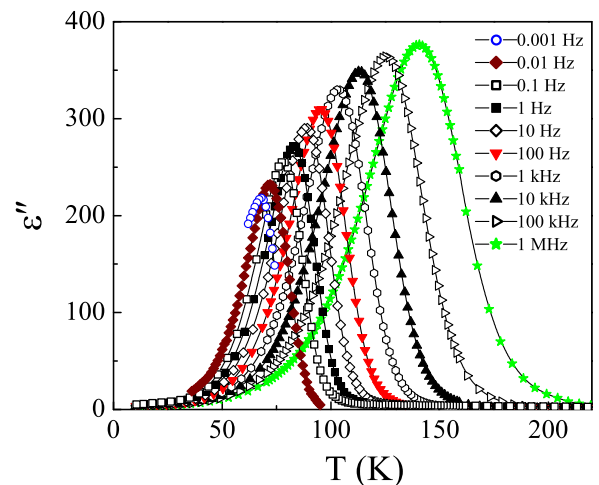

FIG. 2. Temperature dependence of the imaginary part of the complex dielectric constant ε'' in BZT50 at various frequencies, where the peak positions of $\varepsilon''(f,T)$ differ from the peak positions of $\varepsilon'(f,T)$ (see Fig. 1).
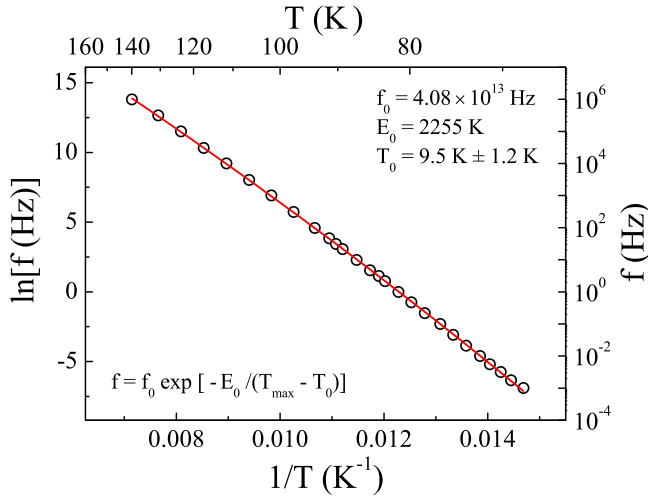
FIG. 3. The temperature $T_{\max}(f)$, at which the maxima of $\varepsilon''(f,T)$ occur, is found empirically to scale with f according to the Vogel-Fulcher (VF) relation $f = f_0 \exp[-E_0/(T_{\max} - T_0)]$ with a VF freezing temperature $T_0 = 9.5 \pm 1.2$ K, attempt frequency $f_0 = 4.08 \times 10^{13}$ Hz, and activation energy $E_0 = 2225$ K.

frequencies f appear. A common method to determine the freezing temperature T_F from the dielectric data is based on the observation that both $\varepsilon'(f,T)$ and $\varepsilon''(f,T)$ show maxima as functions of temperature. For example, the temperature $T_{\max}(f)$ at which the maximum of $\varepsilon'(f,T)$ or $\varepsilon''(f,T)$ occurs has been found empirically to scale with f according to the Vogel-Fulcher (VF) relation

$$f = f_0 \exp[-E_0/(T_{\max} - T_0)], \qquad (1)$$

where f_0, E_0, and T_0 are parameters of the system. The VF relation (1) is applicable to both relaxors [5] and dipolar glasses [29]. Usually the maxima in the temperature dependence of the imaginary part of the dielectric constant ε'' are better defined; therefore the freezing temperature has been determined from them. The characteristic relaxation frequency, determined from the peaks in $\varepsilon''(T)$, is plotted in Fig. 3 versus reciprocal temperature, and is found to follow the Vogel-Fulcher law. The parameters f_0, E_0, and T_0 were determined by a best fit analysis to Eq. (1) and are displayed in Fig. 3. Specifically, the value of T_0 is given by $T_0 = 9.5 \pm 1.2$ K, the attempt frequency is $f_0 = 4.08 \times 10^{13}$ Hz, while the activation energy is $E_0 = 2225$ K.

One is obviously tempted to interpret T_0 as the static limit of the freezing temperature T_F; however, there will be in general two different sets of parameters for the real and imaginary parts of the dielectric constant and thus the choice of T_F is not unique.

Some information about the shape of the relaxation spectrum can be obtained from the so-called Cole-Cole diagram, where ε'' is plotted vs ε' in a wide temperature interval, as shown in Fig. 4. The shape of the plots becomes asymmetric at low temperatures, indicating that the dielectric relaxation is strongly polydispersive. In order to extract the relevant parameters, such as the static dielectric constant ε_s and ε_∞,
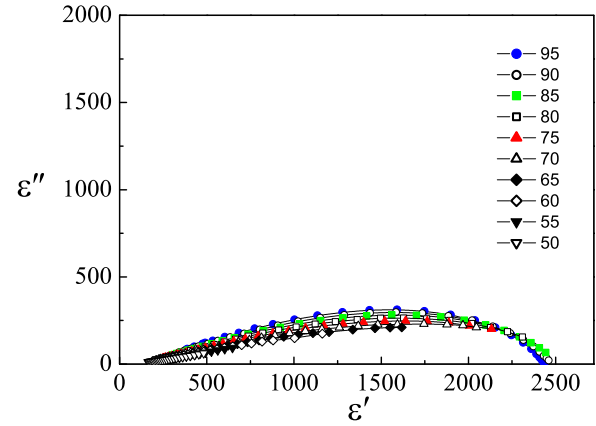

FIG. 4. Cole-Cole diagram: Measured values of ε'' plotted vs ε' in BZT50 at various temperatures between 50 and 95 K. Solid lines between experimental points measured at the same temperature serve as guide to the eye.

we performed a fit to the Havriliak-Negami (HN) function

$$\varepsilon^*(\omega,T) = \varepsilon_\infty + \frac{\varepsilon_s - \varepsilon_\infty}{[1 + (i\omega\tau)^\alpha]^\beta}, \qquad (2)$$

where $\omega = 2\pi f$ and τ is the characteristic relaxation time of the medium. In Fig. 5, ε_s and ε_∞ are plotted as functions of temperature. The HN method yields a reliable estimate for the temperature dependence of the static dielectric constant. On the other hand, the Cole-Cole diagrams show clearly that by lowering the temperature the dielectric relaxation becomes strongly polydispersive, i.e., the dielectric dispersion cannot be completely covered even with a ten decades wide range of frequencies, which was experimentally available. Therefore, the above procedure can provide information about the temperature dependence of relevant parameters ε_s, ε_∞, and τ in a relatively narrow temperature range. We will show later that the static dielectric constant ε_s, determined from the fit of experimental data to HN function, coincide with the values ε_{FC}, determined by a quasistatic FC experiment in low electric field. The FC experiment in low electric field provides the quasistatic FC dielectric constant $\varepsilon_s = \varepsilon_{FC}$, which is not
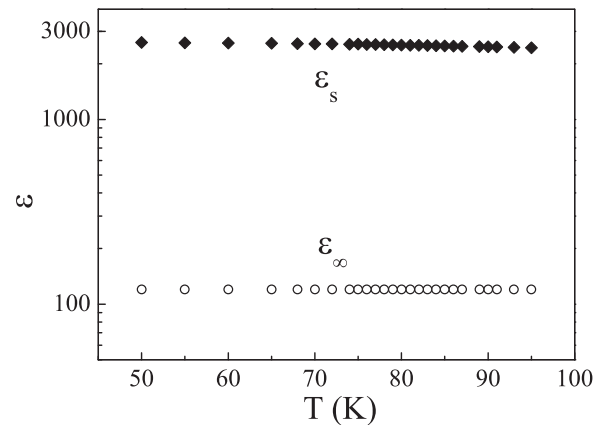

FIG. 5. Temperature dependence of the parameters ε_s and ε_∞ in BZT50. The parameters were obtained by fitting experimental data with the Havriliak-Negami (HN) function.
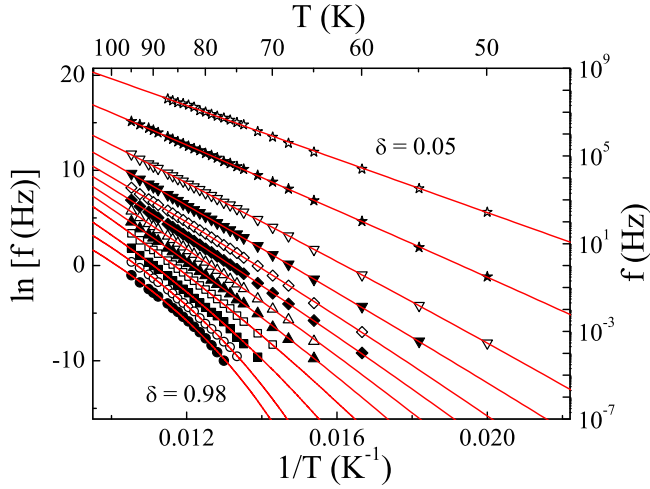
FIG. 6. Temperature-frequency plots for several fixed values of the reduced dielectric constant δ, top to bottom, 0.05, 0.10, 0.20, 0.30, 0.40, 0.50, 0.60, 0.70, 0.80, 0.90, 0.95, 0.98. Solid lines are fits obtained with a generic VF type ansatz, providing a freezing temperature $T_0(\delta)$ for each value of the parameter δ.

experimentally accessible by standard dielectric spectroscopy at low temperatures.

In order to extract the information about the relaxation spectrum from the dielectric data we apply the method of temperature-frequency plots [29,30]. We consider the real part of the dielectric constant ε' and introduce the ratio

$$\delta = \frac{\varepsilon' - \varepsilon_\infty}{\varepsilon_s - \varepsilon_\infty}. \tag{3}$$

The parameter $\delta = \delta(\omega, T)$, where $\omega = 2\pi f$, is determined solely on the basis of experimental values of the dielectric constant. One can always choose a set of fixed values of δ and find the corresponding values of ε' by a suitable interpolation technique. As one scans ε' between ε_s and ε_∞, δ varies between the values 1 and 0. Figure 6 shows the plot for $\log(\omega)$ vs $1/T$ obtained in this way for a set of δ values $0.05 < \delta < 0.98$. One method to analyze these plots is to express δ as an integral over the probability distribution of relaxation times $g[\log(\omega_a \tau)]$, namely,

$$\delta = \int_{z_1}^{z_2} \frac{g(z)dz}{1 + (\omega/\omega_a)^2 \exp(2z)}, \tag{4}$$

where $z = \log(\omega_a \tau)$, with ω_a representing an arbitrary unit frequency, and z_1 and z_2 correspond to the cutoff limits of the relaxation spectrum [29]. Here δ contains mainly contributions of $g(z)$ for relaxation times below $1/\omega$. To explicitly calculate the integral in Eq. (4) one must make a specific ansatz for the probability distribution function $g(z)$ and for the temperature dependence of the two integration limits z_1 and z_2, and then fit these to the data.

Alternatively, it is also possible to extract the relaxation parameters directly from the temperature-frequency plots by fitting each curve with a generic VF type ansatz

$$\log(\omega \tau_{0i}) = -E_i/(T - T_{0i}), \tag{5}$$

where i refers to the ith curve in the plot [31]. This then leads to a VF type temperature dependence of the ith relaxation time
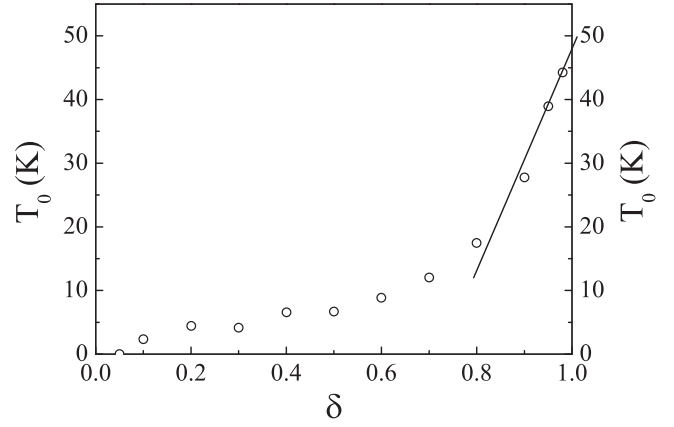

FIG. 7. Freezing temperature T_0 vs δ. The limiting cases $\delta \to 1$ and $\delta \to 0$ yield the freezing temperatures $T_{02} = 48.1$ K and $T_{01} \approx 0$ K, respectively. Solid line is extrapolation to $\delta \to 1$. The value $T_0 = 9.5$ K determined from the maxima of $\varepsilon''(f,T)$ (see Fig. 3) approximately corresponds to $\delta \approx 0.6$.

$\tau_i = 1/(2\pi f_i)$, namely, $\tau_i = \tau_{0i} \exp[E_i/(T - T_{0i})]$, or

$$f_i = f_{0i} \exp[-E_i/(T - T_{0i})]. \tag{6}$$

By fitting Eq. (6) to the δ plots in Fig. 6 we obtain a set of freezing temperatures corresponding to all intermediate values of δ, as shown in Fig. 7. The limiting cases $\delta \to 1$ and $\delta \to 0$ then yield the parameters for the longest and shortest relaxation time, respectively, i.e., $T_{02} = 48.1$ K, $E_{02} = 725$ K, and the attempt frequency $f_{02} = 3.65 \times 10^5$ Hz, and $T_{01} \approx 0$ K, $E_{01} = 1330$ K, and the attempt frequency $f_{01} = 2.17 \times 10^{14}$ Hz.

One of the fundamental experiments to probe the glassy/relaxor nature of the material under investigation is to measure the splitting between the FC and ZFH susceptibility [2]. Figure 8 shows the temperature dependence of the FC and ZFH (after field-cooled) quasistatic dielectric polarization. The highest dc electric field in the FC experiment was 28 kV/cm
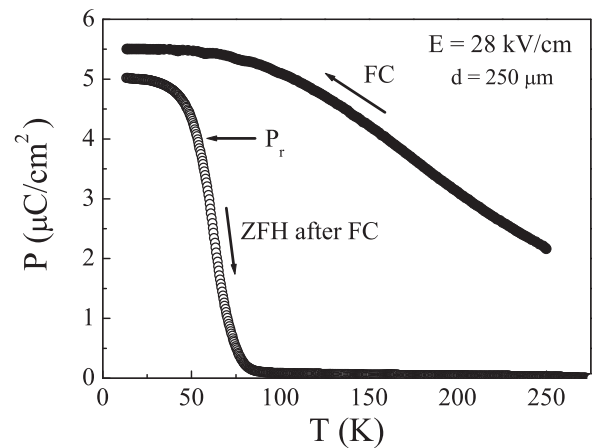

FIG. 8. Temperature dependence of the FC and ZFH (after field-cooled) quasistatic dielectric polarization in high electric field (28 kV/cm). There is no sign of an induced ferroelectric phase. The ZFH polarization represents the remanent polarization P_r. As indicated, the steepest slope in $P_r(T)$ variation, at $T_F \sim 50$ K, yields an estimate for the freezing temperature.

(700 V across 250 μm thick sample). The ZFH (after field-cooled) polarization represents the remanent polarization P_r, because the external electric field (in a FC experiment) was removed from the sample at the lowest temperature.

The experiment presented in Fig. 8 can also provide an estimate for the freezing temperature T_F. P_r remains nearly frozen up to temperatures where most of the relaxation spectrum remains frozen. It is thus expected that the highest rate of relaxation of P_r would take place close to the freezing temperature, $T_{02} \sim 48.1$ K, as indeed indicated by the steepest slope in $P_r(T)$ variation, shown in Fig. 8. It should be noted, however, that the freezing temperature $T_F \sim 50$ K thus obtained is not a true static quantity, but rather depends on the experimental time scale defined by the rate of the temperature scan in the ZFH experiment (+1.6 K/min). We may conclude that the results shown in Fig. 8 represent strong evidence that the state of BZT50 in high external electric fields is indeed analogous to a spin-glass state [6].

In order to decide whether BZT50 is a relaxor or a dipolar glass we have investigated the relation $P(E)$ between the induced polarization and the applied quasistatic electric field. The external field was applied to the sample from 0 up to 28 kV/cm, and conversely, with a rate of approximately 0.002 Hz. The polarization measurements were performed always after cooling the sample from room temperature to a desired temperature (in zero electric field) with a cooling rate of -1.6 K/min. In a relaxor, "slim" ferroelectric hysteresis loops with a nonzero remanent polarization are typically observed below the freezing temperature T_F, and large "square" loops appear in certain symmetry directions for large fields [26]. Above T_F, where the polar nanoclusters are dynamic, the remanent polarization approaches zero, but the $P(E)$ relation is nonlinear [32]. This is not the case in dipolar glasses, where the basic reorientable units are either isolated dipoles or small polar nanoregions, and the formation of domains in the applied field does not occur. In a relaxor, however, the basic reorientable units are polar nanoregions, where the dipole moments are sufficiently large so that the system can order ferroelectrically in a large external field. The remanent polarization is due to the fact that frozen-out polar nanoregions orient in the applied electric field, and that part of this order remains when the field is turned off. The nanoregions interact with each other, and therefore it may take a long time before this induced orientational order decays to zero.

Figure 9 shows the relation between the induced polarization and the applied field at several temperatures above T_F for which the applied frequency can still be considered as quasistatic. Note the nonlinear relation $P(E)$ with zero remanent polarization at all temperatures. With decreasing temperature the nonlinearity increases. It might be possible that the electric field of 28 kV/cm (dc or ac external voltage), which was used in BZT50 experiments, was not high enough to induce a ferroelectric phase. However, by our knowledge, in all relaxor ferroelectrics studied so far, the electric field necessary to induce the ferroelectric phase has been by almost an order of magnitude smaller than the one used in BZT50 experiments. Due to experimental limitations the maximum applied field was up to 28 kV/cm.

Figure 10 shows the results of the fitting of the nonlinear $P(E)$ relation to a simple expansion $P(E) = \varepsilon_0\varepsilon_1 E + \varepsilon_3 E^3 +$
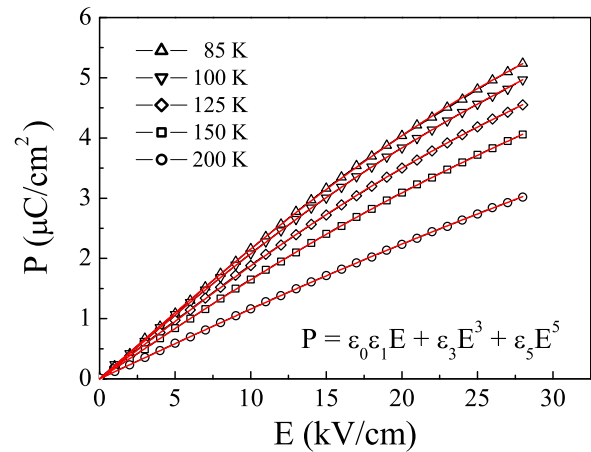

FIG. 9. Relation between the induced polarization and the applied quasistatic electric field $P(E)$ at several temperatures above T_F. Note the nonlinear relation $P(E)$ with zero remanent polarization at all temperatures. With decreasing temperature the nonlinearity increases.

$\varepsilon_5 E^5$, introducing the first, third, and fifth order dielectric constants. The third order dielectric constant ε_3 is negative, and is responsible for the lowering of the induced dielectric polarization in a dc electric field.
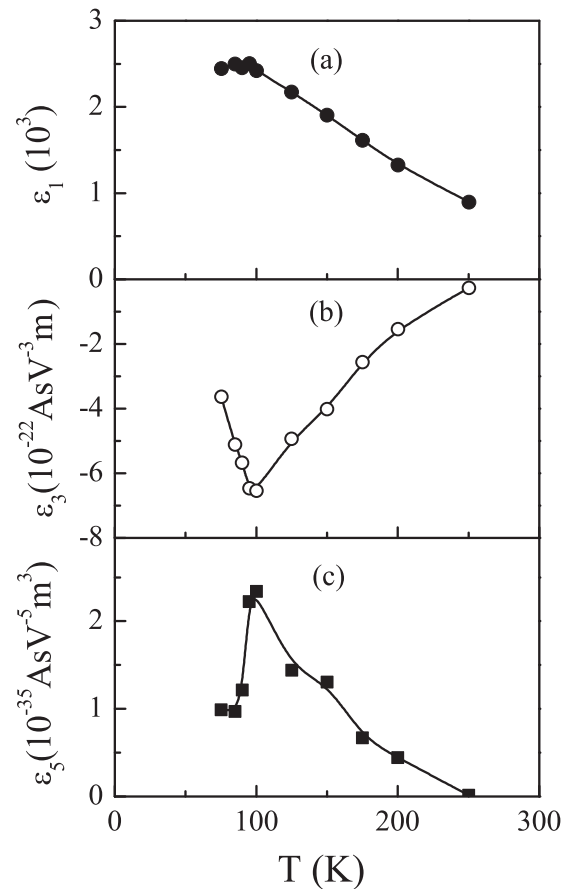

FIG. 10. Temperature dependence of the first (a), third (b), and fifth (c) order dielectric constants obtained by fitting of the nonlinear $P(E)$ data with the function $P(E) = \varepsilon_0\varepsilon_1 E + \varepsilon_3 E^3 + \varepsilon_5 E^5$.
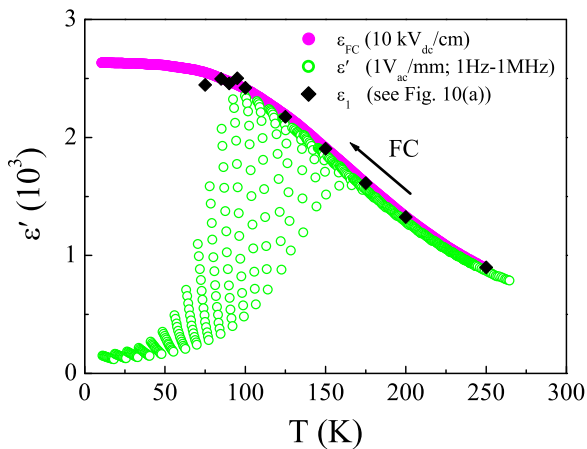
FIG. 11. Temperature dependence of the dielectric constant $\varepsilon_{FC} \cong P(E)_{FC}/(\varepsilon_0 E)$ obtained by a field-cooled experiment in low electric field (10 kV/cm). ε_{FC} values (diamonds) agree well with the values of ε_1 shown in Fig. 10(a). Also presented (open circles) is the temperature and frequency dependence (1 Hz–1 MHz) of the real part of dielectric constant $\varepsilon'(f,T)$ measured in a low electric field (1 V/mm).

Figure 11 shows the temperature dependence of the dielectric constant ε_{FC}, which was obtained by a field cooled experiment, where a dc field of 10 kV/cm was applied to the BZT50 sample and the quasistatic dielectric polarization was measured on cooling. The cooling rate was −1.6 K/min, i.e., the same as in all FC experiments (cf. Fig. 8). From the results presented in Fig. 9 it is known that the relationship between polarization and electric field $P(E)$ is nonlinear at high electric fields. However, at low fields ($E \lesssim 10$ kV/cm) the system is still in the linear regime, which means that it is possible to determine the dielectric constant ε_{FC} from the measured polarization using the simple linear relation $P(E) \cong \varepsilon_0 \varepsilon E$. The temperature dependence of ε_{FC} is displayed in Fig. 11. The linear dielectric constant values thus obtained agree well with the values of ε_1 shown in Fig. 10(a).

Also presented in Fig. 11 is the temperature dependence of the real part of the dynamic dielectric constant $\varepsilon'(f,T)$ measured at different frequencies (0.001 Hz–1 MHz) with a low electric field amplitude of 1 V/mm. As already displayed in Fig. 1, $\varepsilon'(f,T)$ shows a typical relaxor behavior in a broad temperature interval, where the maxima in ε' at different frequencies occur. Figure 11 demonstrates that the quasistatic FC experiment in low electric field yields the static FC dielectric constant $\varepsilon_s = \varepsilon_{FC}$ at low temperatures, which is not experimentally accessible by standard dielectric spectroscopy. Above $T \sim 100$ K, however, ε_{FC} coincides with the peaks in the dynamic dielectric constant $\varepsilon'(f,T)$.

The linear field-cooled susceptibility $\chi_1 = \varepsilon_1 - 1$ in relaxors and dipolar glasses, and in related systems can be generally written in the form [33]

$$\chi_1 = \frac{C(1-q)}{T - T_C(1-q)}, \tag{7}$$

where C and T_C represent the Curie constant and temperature, respectively, and $q = q(T)$ is the spin-glass or Edwards-Anderson (EA) order parameter. The parameters C and T_C

can be determined from χ_1 measured in the asymptotic regime at high temperatures, where Eq. (7) reduces to the well-known Curie-Weiss law $\chi_1 \cong C/(T - T_C)$. The linear susceptibility for BZT50 was extracted from the field-cooled polarization according to $\chi_1 \cong P(E)/(\varepsilon_0 E)$, where $P(E)$ was measured in the same manner as in Fig. 9, but with a much smaller field amplitude $E \lesssim 10$ kV/cm, so that a linear regime of $P(E)$ was warranted. The parameter values are $C = 1.424 \times 10^5$ K and $T_C = 124.6$ K. The EA order parameter has then been calculated from Eq. (7) by using the data for χ_1 in the low temperature regime. The result for BZT50 is shown in Fig. 12. Note that the EA order parameter $q(T)$ is a typical decreasing function of temperature, which vanishes in the asymptotic high temperature regime.

Since BZT50 has many features which are characteristic for relaxors, we can tentatively describe the system in terms of the spherical random bond–random field (SRBRF) model of relaxors [34]. This could be justified microscopically by assuming that the elementary dipolar units are not just isolated off-center Ti^{4+} ions, but some clustering of the elementary dipoles may occur [12,13]. Hence, unlike the case of typical dipolar glasses, the dipolar degrees of freedom cannot be described by fixed-length pseudospins, but rather as vectors of variable length as in the SRBRF model. According to the SRBRF model, the order parameter q satisfies the equation

$$q = (J/T)^2(1-q)^2(q + \Delta/J^2), \tag{8}$$

where the parameter J represents the half-width of the Gaussian distribution of random interactions (bonds), and Δ is the variance of the distribution of local random electric fields. By fitting this equation to the experimental data for $q(T)$ in Fig. 12, we obtain the following values for the parameters: $J = 165.75$ K, $\Delta/J^2 = 0.025$. Note that J is larger than the average random interaction $J_0 \equiv T_C = 124.6$ K, which is the condition for the absence of long range order in zero field in relaxors.
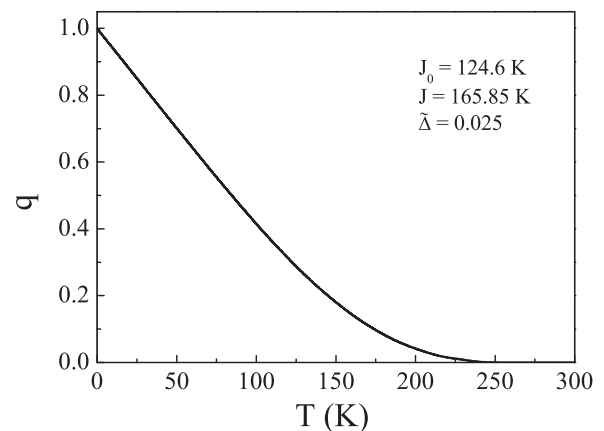

FIG. 12. Temperature dependence of the spin-glass or Edwards-Anderson (EA) order parameter $q(T)$ derived from Eq. (7), where the linear susceptibility has been determined from the field-cooled polarization measured in low electric field (Fig. 11). Also displayed are the values of the fit parameters J_0, J, and $\tilde{\Delta} = \Delta/J^2$ obtained by fitting Eq. (8) to $q(T)$.

The fact that $q(T)$ obeys Eq. (8), which has been derived for a typical lead based heterovalent relaxor system, suggests that BZT50 is characterized by yet another relaxor feature. However, it should be remembered that a field-induced ferroelectric state cannot be induced by cooling in a large electric field. Hence, BZT50 can be tentatively classified as a dipolar glass with a number of relaxor features. This is consistent with the observed negative value of the third order static dielectric nonlinearity, which technically prevents the system from reaching a field-induced ferroelectric state [35]. It should be noted that BZT is available only as ceramics and no single crystals seem to exist. Thus it is possible that for a symmetry direction in a single crystal BZT50 a field-induced ferroelectric phase would exist; however, when averaged over all grain orientations in a ceramics this feature could disappear.

IV. CONCLUSIONS

It is widely accepted that the BaZr$_x$Ti$_{1-x}$O$_3$ (BZT) solid solution for concentrations $0.25 \lesssim x \lesssim 0.75$ behaves as a lead-free isovalent relaxor system. However, there have been recent arguments that BZT should be classified as a dipolar glass rather than a typical relaxor. The present dielectric spectroscopy study has revealed a number of relaxor features of BZT50. Specifically, the real part of the complex permittivity has been analyzed by means of the temperature-frequency plots, which shows that the relaxation times of each segment of the spectrum obey the Vogel-Fulcher relation, except for the high frequency limit where the familiar Arrhenius law applies. Since these features in principle appear both in relaxors and dipolar glasses, the question whether BZT50 is a relaxor or a dipolar glass cannot be answered by these findings alone. A more decisive experiment is the measurement of the dielectric polarization $P(E)$ in an applied quasistatic electric field. For large fields the relation $P(E)$ is nonlinear, but it is not possible to induce a ferroelectric phase, which would be a distinctive feature of relaxor behavior. Moreover, the third order nonlinear dielectric constant turns out to be negative, whereas in relaxors it is expected to be positive. Thus the

$P(E)$ experiment supports the dipolar glass picture for BZT50 as found in relaxors below the critical electric field E_c and at high temperatures.

From the linear dielectric susceptibility the spin-glass or Edwards Anderson (EA) order parameter $q(T)$ has been determined. Again, the EA order parameter has a typical decreasing temperature profile, which could be interpreted either as a relaxor or dipolar glass feature. It turns out, however, that $q(T)$ can be described by the theoretical model of relaxors, which is based on the concept of interacting polar nanoregions. Polar nanoregions seem to exist in BZT50 and are presumably due to the clustering of individual Ti^{4+} dipoles. However, these polar clusters are too small to enable the formation of macroscopic domains in an applied field, which would lead to large "square" hysteresis loops as seen in typical relaxors.

Thus we may conclude that the BZT50 ceramic sample has a number of properties that can be found in relaxor systems. On the one hand, the high dielectric constant observed in BZT50 is typically observed in canonical relaxor systems like lead magnesium niobate (PMN) in which the ferroelectric state can be induced by the electric field. In contrast to PMN, the electric field does not have a significant impact on the dielectric dispersion and the relaxation times in BZT50 ceramics. In addition, no ferroelectric state can be induced in BZT50 with fields up to the 28 kV/cm, which is an order of magnitude higher than typical critical fields observed in other canonical relaxor systems. On the other hand, such properties as the nonlinear $P(E)$ profile, negative ε_3, and glassy dynamics with divergent maximum relaxation time are typical for dipolar glasses; however, they can also be found in the dipolar glass section of the E-T phase diagram of relaxors. This indicates that BZT50 behaves like an *incipient* relaxor system, where a ferroelectric state cannot be induced by application of a static electric field down to the lowest temperatures.

[1] R. Blinc, *Advanced Ferroelectricity* (Oxford University Press, New York, 2011).

[2] A. Levstik, Z. Kutnjak, C. Filipič, and R. Pirc, Phys. Rev. B **57**, 11204 (1998).

[3] G. A. Smolenskii and V. A. Isupov, Dokl. Akad. Nauk SSSR **9**, 652 (1954).

[4] L. E. Cross, Ferroelectrics **76**, 241 (1987); **151**, 305 (1994).

[5] G. A. Samara, in *Solid State Physics*, edited by H. Ehrenreich and R. Spaepen (Academic, New York, 2001), Vol. 56, p. 1.

[6] D. Sherrington, Phys. Rev. Lett. **111**, 227601 (2013).

[7] R. Farhi, M. El Marssi, A. Simon, and J. Ravez, Eur. Phys. J. B **9**, 599 (1999).

[8] T. Maiti, R. Guo, and A. S. Bhalla, J. Am. Ceram. Soc. **91**, 1769 (2008).

[9] T. Maiti, R. Guo, and A. S. Bhalla, Appl. Phys. Lett. **89**, 122909 (2006).

[10] T. Maiti, R. Guo, and A. S. Bhalla, J. Appl. Phys. **100**, 114109 (2006).

[11] T. Maiti, R. Guo, and A. S. Bhalla, Ferroelectrics **425**, 4 (2011).

[12] J. Petzelt, D. Nuzhnyy, V. Bovtun, M. Kempa, M. Savinov, S. Kamba, and J. Hlinka, Phase Trans. **88**, 320 (2014).

[13] J. Petzelt, D. Nuzhnyy, M. Savinov, V. Bovtun, M. Kempa, T. Ostapchuk, J. Hlinka, G. Canu, and V. Buscaglia, Ferroelectrics **469**, 14 (2014).

[14] D. Nuzhnyy, J. Petzelt, M. Savinov, T. Ostapchuk, V. Bovtun, M. Kempa, J. Hlinka, V. Buscaglia, M. T. Buscaglia, and P. Nanni, Phys. Rev. B **86**, 014106 (2012).

[15] W. Kleemann, S. Miga, J. Dec, and J. Zhai, Appl. Phys. Lett. **102**, 232907 (2013).

[16] X.-S. Qian, H.-J. Ye, Y.-T. Zhang, H. Gu, X. Li, C. A. Randall, and Q. M. Zhang, Adv. Funct. Mater. **24**, 1300 (2014).

[17] W. Kleemann, J. Dec, and S. Miga, Phase Trans. **88**, 234 (2015).

[18] A. R. Akbarzadeh, S. Prosandeev, E. J. Walter, A. Al-Barakaty, and L. Bellaiche, Phys. Rev. Lett. **108**, 257601 (2012).

[19] S. Prosandeev, D. Wang, A. R. Akbarzadeh, B. Dkhil, and L. Bellaiche, Phys. Rev. Lett. **110**, 207601 (2013).

[20] S. Prosandeev, D. Wang, and L. Bellaiche, Phys. Rev. Lett. **111**, 247602 (2013).

[21] D. Wang, J. Hlinka, A. A. Bokov, Z.-G. Ye, P. Ondrejkovic, J. Petzelt, and L. Bellaiche, Nat. Commun. **5**, 5100 (2014).

[22] J. Macutkevic, J. Banys, R. Grigalaitis, and Yu. Vysochanskii, Phys. Rev. B **78**, 064101 (2008).

[23] J. Banys, R. Grigalaitis, A. Mikonis, J. Macutkevich, and P. Keburis, Phys. Status Solidi C **6**, 2725 (2009).

[24] A. R. Bishop, A. Bussmann-Holder, S. Kamba, and M. Maglione, Phys. Rev. B **81**, 064106 (2010).

[25] A. Bussmann-Holder, J. Phys.: Condens. Matter **24**, 273202 (2012).

[26] Z. Kutnjak, B. Vodopivec, and R. Blinc, Phys. Rev. B **77**, 054102 (2008).

[27] Z. Kutnjak, R. Pirc, and R. Blinc, Appl. Phys. Lett. **80**, 3162 (2002).

[28] A. Levstik, C. Filipič, Z. Kutnjak, I. Levstik, R. Pirc, B. Tadić, and R. Blinc, Phys. Rev. Lett. **66**, 2368 (1991).

[29] Z. Kutnjak, R. Pirc, A. Levstik, I. Levstik, C. Filipič, R. Blinc, and R. Kind, Phys. Rev. B **50**, 12421 (1994).

[30] Z. Kutnjak, C. Filipič, A. Levstik, and R. Pirc, Phys. Rev. Lett. **70**, 4015 (1993).

[31] Z. Kutnjak, C. Filipič, R. Pirc, A. Levstik, R. Farhi, and M. El Marssi, Phys. Rev. B **59**, 294 (1999).

[32] A. Levstik, V. Bobnar, C. Filipič, J. Holc, M. Kosec, R. Blinc, Z. Trontelj, and Z. Jagličić, Appl. Phys. Lett. **91**, 012905 (2007).

[33] D. Viehland, S. J. Jang, L. E. Cross, and M. Wuttig, Phys. Rev. B **46**, 8003 (1992).

[34] R. Pirc and R. Blinc, Phys. Rev. B **60**, 13470 (1999).

[35] R. Pirc and Z. Kutnjak, Phys. Rev. B **89**, 184110 (2014).